

Fractional Mathematical Model of Covid-19 with Quarantine

Muhammad Rifki Nisardi¹, Kasbawati^{1*}, Khaeruddin¹, Antonin Robinet² and
Khaled Chetehouna²

¹Department of Mathematics, Universitas Hasanuddin, Makassar, Indonesia

²INSA Centre-Val de Loire, Université d'Orléans, PRISME (EA 4229), Bourges, France

Email: kasbawati@unhas.ac.id

Abstract

This study aims to observe the dynamics of the spread of COVID-19 with the SIR-Model by considering the quarantine (Q) scheme. We also involve a fractional order in the model. Then the basic reproduction numbers were calculated using the generation matrix method, analyzed the local stability of the fractional model for each equilibrium point, and observed its relation to the basic reproduction numbers. We perform the sensitivity analysis to see the effect of parameters on changes in the basic reproduction numbers. We applied the Grunwald-Letnikov method for numerical simulations. Estimation for parameters was also carried out on the existing parameters in the model to obtain parameter values that could represent the actual conditions. Furthermore, with a fractional model, we approximated the model to the data of COVID-19 in West Sulawesi, Indonesia, so that we could obtain a fractional order since it could describe the data more accurately.

Keywords: SIR-Q Model; COVID-19; basic reproduction number; Fractional Mathematical Model; Grunwald Letnikov Method.

Abstrak

Penelitian ini bertujuan untuk mengkaji dinamika penyebaran COVID-19 dengan model matematika orde fraksional penyebaran penyakit SIR-Q dengan mempertimbangkan skema karantina (Q) untuk mengendalikan penyebaran COVID-19. Bilangan reproduksi dasar dihitung menggunakan metode matriks generasi. Kemudian, dianalisa kestabilan lokal model fraksional untuk titik kesetimbangan dan lalu dianalisa kaitannya dengan bilangan reproduksi dasar. Analisis sensitivitas dilakukan untuk mengamati pengaruh parameter terhadap perubahan bilangan reproduksi dasar. Simulasi numerik dilakukan dengan menggunakan metode eksplisit Grunwald-Letnikov. Estimasi juga dilakukan terhadap parameter yang ada pada model untuk memperoleh nilai parameter yang merepresentasikan kondisi aktual penyebaran COVID-19 di Sulawesi Barat. Selanjutnya dengan model fraksional dilakukan pendekatan terhadap data kasus aktif COVID-19 di Sulawesi Barat sehingga diperoleh orde fraksional tertentu yang menghasilkan pendekatan nilai kasus aktif COVID-19 yang lebih akurat terhadap real data.

Kata Kunci: Model SIR-Q; COVID-19; bilangan Reproduksi Dasar; Model Matematika Fraksional; Metode Grunwald-Letnikov.

1. INTRODUCTION

Coronavirus-disease-2019 (COVID-19) is an infectious disease caused by a mutation of a new type of coronaviruses called Severe Acute Respiratory Syndrome Coronavirus 2 (SARS-CoV-2), which appeared in the city of Wuhan, China, in December 2019. The COVID-19 viruses are transmitted through human-to-human. The virus will spread through the droplets of infected COVID-19 by sneezing, coughing, or talking at a close distance [1]. Since the COVID-19 virus appeared, various countries have tried to suppress the spread of the virus with some preventive actions. According to applicable procedures, people should apply health protocols by wearing masks and undergoing quarantine periods.

*) Corresponding author

Submitted December 21st, 2021, Revised March 24rd, 2022, Accepted for publication March 27th, 2022.

©2022 The Author. This is an open-access article under CC-BY-SA license (<https://creativecommons.org/licence/by-sa/4.0/>)

Complex interactions involved in the COVID-19 spreading interest to be modeled using a mathematical approach. A mathematical model is a set of equations or inequalities that describe the behavior of the real problem with given assumptions. Several mathematical models of diseases such as Susceptible-Infectious-Recovered (SIR), Susceptible-Exposed-Infectious-Recovered (SEIR), and Susceptible-Exposed-Infectious-Recovered-Susceptible (SEIRS) have been widely used to model various types of disease spreading along with related assumptions. For example, the spread of TB, Meningitis, Hepatitis, Dengue Fever (DHF), and HIV-AIDS has been studied by some researchers using a mathematical model (see for instance [2]–[9]). Nowadays, mathematical models of COVID-19 have also been focused on by many researchers such as [1], [10]–[14]. In [13], researchers focused on a compartment containing individuals with a higher risk of spreading the virus than usually called super-spreaders. They used a differential equations system with integer-order derivatives on their model. The research on fractional calculus and fractional differential equations has arisen in various fields. It does not only in mathematics but also in physics, engineering, and other applied sciences [15]–[22]. In [16], they used the same model as [13], but the derivatives operator in the model was generalized to be fractional derivatives. It aimed to obtain a better approach to the actual data cases of COVID-19 in Wuhan, Spain, and Portugal. As a result, they obtained different fractional-order values for each region to approximate the data.

In this study, we formulated the SIR mathematical model with a fractional order using the Caputo derivative by considering the quarantine compartment (Q) as an effort to reduce the spread of COVID-19. This article consists of several subsections: the first part is an introduction explaining the urgency of this research. The second part presents the formulation of a mathematical model considering the quarantine scheme. In the third part, the results and discussion of this research are presented. The fourth section contains parameter estimation and numerical simulation by considering various scenarios to determine the effect of several changes. The fifth section is the conclusions of this study.

2. METHODS

2.1. Preliminary work

We first propose a mathematical model describing the natural spread of COVID-19 based on the SIRD model. This model accounts for people who are susceptible to the disease but still sane (S), people who are infected with the disease (I), people who have recovered and for which we assume immunity to further infections (R), and the group of people who have succumbed to the disease (D). No measure to prevent the spread of the disease, such as quarantine or vaccination, is considered. The system of differential equations is as follows:

$$\begin{aligned}\frac{dS}{dt} &= -\beta S \frac{I}{N}, \\ \frac{dI}{dt} &= \beta S \frac{I}{N} - (\mu + \gamma)I, \\ \frac{dR}{dt} &= \gamma I, \\ \frac{dD}{dt} &= \mu I,\end{aligned}$$

where β is the infection rate, γ is the recovery rate, μ is the mortality rate, and N is the total population. Let's consider a test case with an initial population of 10000 sane people on the first day. The parameters have respective values of 0.4, 0.016, and 0.001. We observe the evolution of the different groups over a year (365 discrete steps):

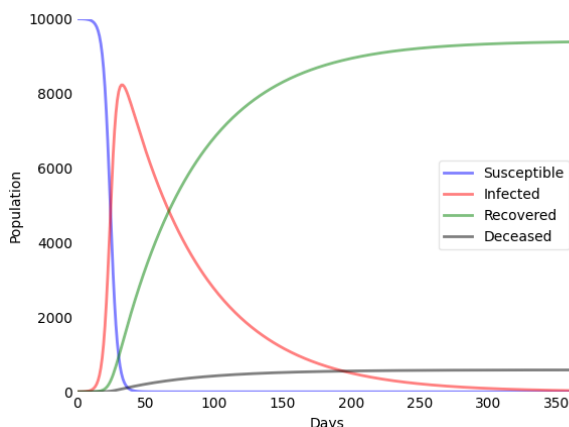


Figure 1. The Dynamics of the SIRD model

We observe a sharp peak of infection in the first days. Within 40 days, there was not a single person that has not been infected with the virus. From here, the number of infected decreases exponentially. We now compute the Sobol indices of the SIRD model using the Monte-Carlo method. We focus on the final number of people that either never have been infected (S_{final}), those who have recovered (R_{final}), and the ones who are deceased (D_{final}). These indices will serve as an estimation of which parameter has the most influence on the evolution of either of these three groups. First, we have to explore a range of parameter values (Table 1). We base our values on the work of Chae et al. 2020 [23]. We ran a total of 10000 simulations.

Table 1. Range of parameter values.

	Ranges	ST_{β}	ST_{γ}	ST_{μ}
S_{final}	$\beta = [0.233 ; 0.462]$	0.720	0.369	0.000
R_{final}	$\gamma = [0.1 ; 0.1667]$	0.627	0.313	0.009
D_{final}	$\mu = [5.10^{-6} ; 1.8.10^{-3}]$	0.020	0.134	0.871

We see that the number of deceased people depends mainly on the mortality rate (0.817), and the same conclusion is drawn for the number of susceptible (0.720). Meanwhile, the number of recovered people also depends on the infection rate (0.627 for β and only 0.313 for γ). We then conclude that to maximize the number of recovered people. We must not find a more effective drug to increase the recovery rate γ but diminish as much as possible the number of infections, hence decreasing the infection rate β . This is the reasoning behind the different sanitary protocols, the strategy of "flattening the curve" and the worldwide vaccination campaign.

2.2. Model Formulation

We propose a mathematical model of the spread of COVID-19 considering a quarantine. It aims to observe how the effect of quarantine controlling the spread of COVID-19 in a population. We

divide the population into four parts based on their health status. Susceptible (S) is individuals who have the probability of being infected with COVID-19; Infected compartment (I), individuals infected with COVID-19; Quarantine compartment (Q), namely individuals undergoing quarantine, both self-quarantine, and hospital treatment. The Recovered compartment (R) is a subpopulation of individuals who have recovered from COVID-19. The interaction among each subpopulation is in Figure 2. It assumed that every individual in the population has the same probability of being infected with COVID-19. There is also no migration of individuals into and out of the system.

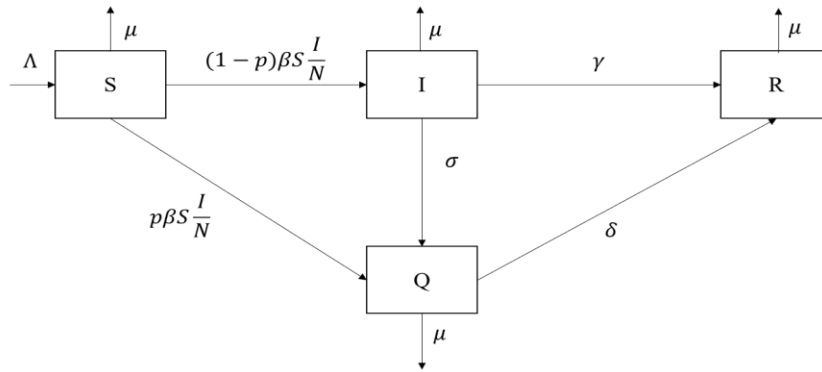


Figure 2. The diagram of the COVID-19 spread model with a quarantine scheme.

Figure 2 shows the dynamics of the spread of COVID-19 disease with a quarantine scheme. Population S increased due to natural births in a population with a birth rate Λ . The S population decreased due to natural deaths experienced by individuals in a population with individual mortality rates (μ) and an individual who has been contacted with infected COVID-19.

Individuals detected (tracing) would move to the quarantine compartment Q with a tracing proportion p , the rest $(1 - p)$ would move to the infected subpopulation I . The subpopulation of infected I increased due to interactions between susceptible individuals and infected individuals who did not trace. Then population I decreased due to natural deaths with the rate (μ), individuals who were declared cured with a cure rate (γ), and individuals who moved to the quarantine compartment with the rate (σ).

The quarantine population (Q) increased due to interactions among susceptible individuals and individuals infected and traced positive for COVID-19 with a proportion of p . Then the population Q decreased due to natural deaths with the rate (μ) and individuals who were declared cured with a cure rate (δ). The recovered population (R) increased due to individuals who recovered from the infected compartment (I) and the quarantine compartment (Q). Then the population Q decreased due to the natural death rate (μ). Based on the assumptions and the interactions among compartments in Figure 1, the model is given in the following system:

$$\begin{aligned} \frac{dS}{dt} &= \Lambda - \mu S - \beta S \frac{I}{N}, \\ \frac{dI}{dt} &= (1 - p)\beta S \frac{I}{N} - (\sigma + \mu + \gamma)I, \\ \frac{dQ}{dt} &= p\beta S \frac{I}{N} + \sigma I - \mu Q - \delta Q, \end{aligned} \tag{1}$$

$$\frac{dR}{dt} = \gamma I - \delta Q - \mu R,$$

where N is the total population. The initial values of all variables are

$$S(0) = S_0, I(0) = I_0, Q(0) = Q_0, R(0) = R_0,$$

where $S_0, I_0, Q_0, R_0 \geq 0$. We assume that all parameters are positive.

Table 2. Parameter of the Model (1).

Parameters	Description
Λ	The natural birth rate in time unit
μ	Rate of natural birth/death.
β	Rate of transmission contact.
p	The proportion of Tracing Contact
σ	The transmission rate of infected to quarantine
γ	The recovery rate of infected
δ	The recovery rate of quarantined

2.3. Fractional Derivative Theory

Definition 1. Riemann-Liouville Fractional Integral [24].

Suppose $f \in L^1[0, \infty)$. For $t > 0$, the fractional integral of Riemann-Liouville with order $\alpha \geq 0$ is defined by

$$I^\alpha f(t) = \frac{1}{\Gamma(\alpha)} \int_0^t (t-x)^{\alpha-1} f(x) dx,$$

$$I^0 f(t) = f(t).$$

Definition 2. Riemann-Liouville Fractional Derivative [25].

Let $\alpha \in \mathbb{R}_+$, a fractional derivative of Riemann-Liouville ${}^{RL}D_t^\alpha$ is defined by

$${}^{RL}D_t^\alpha f(t) = D^n I_a^{n-\alpha} f(t),$$

$$= \frac{1}{\Gamma(n-\alpha)} \frac{d^n}{dt^n} \left(\int_a^t (t-x)^{n-\alpha-1} f(x) dx \right), \quad t > a,$$

where n is the smallest natural number greater than α , $n-1 \leq \alpha < n$.

Definition 3. Caputo Fractional Derivative [26]

Let $\alpha > 0, t > 0$, and $n \in \mathbb{N}$, Caputo fractional derivative ${}_0^C D_t^\alpha := \frac{d^\alpha}{dt^\alpha}$ with order α for $f(t)$ is defined by:

$${}_0^C D_t^\alpha f(t) = \begin{cases} \frac{1}{\Gamma(n-\alpha)} \int_0^t (t-x)^{n-\alpha-1} f^{(n)}(x) dx, & n-1 < \alpha < n, \\ f^{(n)}(t), & \alpha = n. \end{cases}$$

Definition 4. Locally asymptotically stable [27].

A system is locally asymptotically stable near or at equilibrium point \bar{x} if there is an $M > 0$ such that $\|x(0) - \bar{x}\| \leq M \Rightarrow x(t) \rightarrow \bar{x}$ as $t \rightarrow \infty$.

Theorem 1. Local stability of Fractional differential system [26], [28], [29].

Let ${}^C_0D_t^\alpha \mathbf{x}(t) = f(\mathbf{x})$, $0 < \alpha \leq 1$, dan $\mathbf{x} \in \mathbb{R}^n$, is a nonlinear fractional differential system. The equilibrium $\bar{\mathbf{x}}$ is the solution of $f(\mathbf{x}) = 0$. This equilibrium $\bar{\mathbf{x}}$ is locally asymptotically stable if for all eigenvalue $\lambda_{(j=0,1,\dots,n)}$ of Jacobian Matrix $\mathbf{A} = \frac{\partial f}{\partial \mathbf{x}}$ in $\bar{\mathbf{x}}$ satisfy $|\arg(\lambda_j)| > \frac{\alpha\pi}{2}$.

Definition 5. Sensitivity Analysis [3]

The normalization of the sensitivity index was obtained by normalizing the variable V , which is differentiable on the parameter p , defined as follows:

$$C_p^V = \frac{\partial V}{\partial p} \times \frac{p}{V}.$$

3. RESULTS AND DISCUSSIONS

3.1. Fractional Model Formulation

Consider that ${}^C_0D_t^\alpha$ is defined as Caputo fractional derivative with order α ($0 < \alpha < 1$). Therefore, system (1) can be rewritten as

$$\begin{aligned} {}^C_0D_t^\alpha(S) &= \Lambda - \mu S - \beta S \frac{I}{N}, \\ {}^C_0D_t^\alpha(I) &= (1 - p)\beta S \frac{I}{N} - (\sigma + \mu + \gamma)I, \\ {}^C_0D_t^\alpha(Q) &= p\beta S \frac{I}{N} + \sigma I - \mu Q - \delta Q, \\ {}^C_0D_t^\alpha(R) &= \gamma I - \delta Q - \mu R. \end{aligned}$$

By assuming new dimensionless variables, $x_1 = \frac{S}{N}$, $x_2 = \frac{I}{N}$, $x_3 = \frac{Q}{N}$, $x_4 = \frac{R}{N}$, the dimensionless model is obtained as follows

$$\begin{aligned} {}^C_0D_t^\alpha(x_1) &= \Lambda - \mu x_1 - \beta x_1 x_2, \\ {}^C_0D_t^\alpha(x_2) &= (1 - p)\beta x_1 x_2 - (\sigma + \mu + \gamma)x_2, \\ {}^C_0D_t^\alpha(x_3) &= p\beta x_1 x_2 + \sigma x_2 - \mu x_3 - \delta x_3, \\ {}^C_0D_t^\alpha(x_4) &= \gamma x_2 - \delta x_3 - \mu x_4, \end{aligned} \tag{2}$$

with initial values of system (2) is non-negative

$$x_1(0) \geq 0, x_2(0) \geq 0, x_3(0) \geq 0, x_4 \geq 0.$$

3.2. The Equilibrium Point of the Fractional Model

The equilibrium point is a solution of the systems that do not change with time. There are two equilibrium points in a model (2), the disease-free equilibrium point and the endemic equilibrium point. The equilibrium point for the Caputo fractional model (2) is when [30], [31]

$${}_0^C D_t^\alpha(x_1) = {}_0^C D_t^\alpha(x_2) = {}_0^C D_t^\alpha(x_3) = {}_0^C D_t^\alpha(x_4) = 0.$$

The disease-free equilibrium point means disease does not spread in a population. This condition occurs when $x_2 = 0$. It means there are no infected individuals that can transmit COVID-19 to others. We obtain the disease-free equilibrium point (E_0) for system (2):

$$E_0 = (x_1^0, x_2^0, x_3^0, x_4^0) = (1, 0, 0, 0).$$

In addition, there is also an endemic equilibrium point. The endemic equilibrium point is the condition when $x_2 \neq 0$. It means that individuals are infected and can transmit COVID-19 to other individuals. The endemic equilibrium point is denoted by

$$E_1 = (x_1^*, x_2^*, x_3^*, x_4^*),$$

with $x_1^* = \frac{\mu}{\mu + \beta x_2^*}$, $x_2^* = \frac{\beta(1-p)\mu - \mu(\sigma + \mu + \gamma)}{\beta(\sigma + \mu + \gamma)}$, $x_3^* = \frac{p\beta\mu + \mu\sigma x_2^* + \beta\sigma(x_2^*)^2}{(\mu + \delta)(\mu + \beta x_2^*)}$, and $x_4^* = \frac{\gamma}{\mu} x_2^* - \frac{\delta(p\beta\mu + \mu\sigma x_2^* + \beta\sigma(x_2^*)^2)}{\mu(\mu + \delta)(\mu + \beta x_2^*)}$.

3.3. Basic Reproduction Number

The basic reproduction number was determined using the Next Generation Matrix (NGM) method [24][26]. Suppose $F_i(x)$ is the rate of addition of new infections in compartment i and $V_i(x)$ is the rate of movement of individuals in compartment i , so that we obtain $F_i(x)$ and $V_i(x)$ as follows:

$$F_i = \begin{pmatrix} (1-p)\beta x_1 x_2 \\ p\beta x_1 x_2 \end{pmatrix}, \tag{3}$$

$$V_i = \begin{pmatrix} \sigma x_2 + \mu x_2 + \gamma x_2 \\ \mu x_3 + \delta x_3 - \sigma x_2 \end{pmatrix}. \tag{4}$$

From equations (3) and (4), it can be obtained matrices F and V which are evaluated at E_0 as follows:

$$F = \frac{\partial F_i}{\partial(x_2, x_3)} = \begin{pmatrix} (1-p)\beta x_1 & 0 \\ p\beta x_1 & 0 \end{pmatrix}_{x_1=x_1^0} = \begin{pmatrix} (1-p)\beta & 0 \\ p\beta & 0 \end{pmatrix},$$

$$V = \frac{\partial V_i}{\partial(x_2, x_3)} = \begin{pmatrix} \sigma + \mu + \gamma & 0 \\ -\sigma & \mu + \delta \end{pmatrix}.$$

Then, we get the inverse of matrix V ,

$$V^{-1} = \begin{pmatrix} \frac{1}{(\sigma + \mu + \gamma)} & 0 \\ \frac{\sigma}{(\sigma + \mu + \gamma)(\mu + \delta)} & \frac{1}{(\mu + \delta)} \end{pmatrix}.$$

Furthermore, from the matrix F and the inverse of V , we obtain the generation matrix,

$$FV^{-1} = \begin{pmatrix} (1-p)\beta & 0 \\ p\beta & 0 \end{pmatrix} \circ \begin{pmatrix} \frac{1}{(\sigma + \mu + \gamma)} & 0 \\ \frac{\sigma}{(\sigma + \mu + \gamma)(\mu + \delta)} & \frac{1}{(\mu + \delta)} \end{pmatrix} = \begin{pmatrix} \frac{(1-p)\beta}{(\sigma + \mu + \gamma)} & 0 \\ \frac{(1-p)\beta\sigma}{(\sigma + \mu + \gamma)(\mu + \delta)} + \frac{p\beta}{(\mu + \delta)} & 0 \end{pmatrix},$$

which has eigenvalues $\lambda_1 = \frac{(1-p)\beta}{(\sigma+\mu+\gamma)}$, $\lambda_2 = 0$. Since the basic reproduction number is the radius spectral of FV^{-1} , $R_0 = \max\{|\lambda_i|: \lambda_i \text{ eigenvalue of } FV^{-1}\}$, we obtain

$$R_0 = \frac{(1-p)\beta}{(\sigma+\mu+\gamma)}$$

3.4. Local Stability of Equilibrium Points

The local stability analysis for the equilibrium point is given in the following theorem.

Theorem 2. *The COVID-19 free equilibrium point on (2) is locally asymptotically stable for all $\alpha \in (0,1]$ if $R_0 < 1$.*

Proof: If the system (2) is linearized and then evaluated at the equilibrium point E_0 , a Jacobian matrix will be obtained as follows:

$$J(E_0) = \begin{pmatrix} -\mu & 0 & 0 & 0 \\ 0 & (1-p)\beta - (\mu + \sigma + \gamma) & 0 & 0 \\ 0 & p\beta + \sigma & -\mu - \delta & 0 \\ 0 & \gamma & -\delta & -\mu \end{pmatrix}$$

Eigenvalue of $J(E_0)$ is the roots of the characteristic equation

$$(\lambda + \mu)^2(\lambda + \mu + \delta)(\lambda - \beta(1-p) + \mu + \sigma + \gamma) = 0.$$

By solving this characteristic equation, we get eigenvalues $\lambda_{1,2} = -\mu$, $\lambda_3 = -\mu - \delta$ and $\lambda_4 = -a_1$, with $a_1 = -\beta(1-p) + \mu + \sigma + \gamma = (1-R_0)(\mu + \sigma + \gamma)$. Since parameter $\mu, \delta > 0$, so $\lambda_{1,2,3} < 0$ or $|\arg(\lambda_i)| = \pi$. Furthermore, for $0 < \alpha < 1$, it satisfies that $|\arg(\lambda_{1,2,3})| > \frac{\alpha\pi}{2}$. For λ_4 , we can obtain $\lambda_4 < 0$ if $a_1 > 0$. Since $(\mu + \sigma + \gamma) > 0$, then $a_1 > 0$ if $R_0 < 1$. Since $0 < \alpha < 1$, it satisfies that $|\arg(\lambda_4)| = \pi > \frac{\alpha\pi}{2}$. So E_0 is locally asymptotically stable if $R_0 < 1$. ■

Furthermore, the theorem of local stability of endemic points is given as follows.

Theorem 3. *The Endemic equilibrium point $E_1 = (x_1^*, x_2^*, x_3^*, x_4^*)$ in (2) is locally asymptotically stable for all $\alpha \in (0,1]$ if $R_0 > 1$.*

Proof: If the system (2) is linearized and then evaluated at the equilibrium point E_1 , a Jacobian matrix will be obtained as follows:

$$J(E_1) = \begin{pmatrix} -\mu - \beta x_2^* & -\beta \frac{\mu}{\mu + \beta x_2^*} & 0 & 0 \\ (1-p)\beta x_2^* & (1-p)\beta \frac{\mu}{\mu + \beta x_2^*} - (\mu + \sigma + \gamma) & 0 & 0 \\ p\beta x_2^* & p\beta \frac{\mu}{\mu + \beta x_2^*} + \sigma & -\mu - \delta & 0 \\ 0 & \gamma & -\delta & -\mu \end{pmatrix}$$

with $x_2^* = \frac{\beta(1-p)\mu - \mu(\sigma + \mu + \gamma)}{\beta(\sigma + \mu + \gamma)} = \frac{-\mu(1-R_0)(\sigma + \mu + \gamma)}{\beta(\sigma + \mu + \gamma)} = \frac{\mu(R_0-1)}{\beta}$. By substituting x_2^* , we obtain

$$J(E_1) = \begin{pmatrix} -\mu R_0 & -\frac{\beta}{R_0} & 0 & 0 \\ (1-p)\mu(R_0-1) & \frac{(1-p)\beta}{R_0} - (\mu + \sigma + \gamma) & 0 & 0 \\ p\mu(R_0-1) & \frac{p\beta}{R_0} + \sigma & -\mu - \delta & 0 \\ 0 & \gamma & -\delta & -\mu \end{pmatrix}.$$

Eigenvalue of the matrix $J(E_1)$ is the roots of the characteristic equation

$$\frac{1}{R_0}(\lambda + \mu + \delta)(\lambda + \mu)(R_0\lambda^2 + (\mu R_0^2 + (\mu + \sigma + \gamma)R_0 - (1-p)\beta)\lambda + \mu(\mu + \sigma + \gamma)R_0^2 - (1-p)\beta\mu) = 0.$$

By solving this characteristic equation, we get eigenvalues $\lambda_1 = -\mu - \delta, \lambda_2 = -\mu$, and the others are obtained from the roots of polynomial

$$\lambda^2 + a_1\lambda + a_2 = 0, \tag{6}$$

with $a_1 = \mu R_0$ and $a_2 = \mu(\mu + \sigma + \gamma)R_0 - \frac{(1-p)\beta}{R_0}\mu$. Since parameters μ and δ are assumed to be positive, then $\lambda_{1,2} < 0$. So, for all $\alpha \in (0,1]$, $|\arg(\lambda_{1,2})| = \pi > \frac{\alpha\pi}{2}$. Therefore, now the stability of E_1 depends on (6). Since we have $a_1 > 0$, the polynomial (6) does not have a pair of complex roots with a positive real part. Based on Proposition 1 (ii) in [1], equation (6) has to satisfy $a_1, a_2 > 0$. Because $a_1 > 0$, then for a_2 , we get

$$(1-p)\beta \frac{(R_0-1)}{R_0} > 0.$$

For all $\alpha \in (0,1]$, we have $a_2 > 0$ if $R_0 > 1$. It implies $|\arg(\lambda_{3,4})| = \pi > \frac{\alpha\pi}{2}$. So, E_1 is locally asymptotically stable if $R_0 > 1$. ■

3.5. Sensitivity Analysis

In this section, we analyzed the sensitivity of the basic reproduction numbers. We observed the effect of the parameter change on the basic reproduction numbers. We also analyzed the effect of changing two parameters on the basic reproduction numbers. Later, the parameter value change could be adjusted based on the problem. Let us consider the following analysis.

- The sensitivity of parameter β with respect to R_0 is defined as,

$$C_\beta^{R_0} = \frac{\partial R_0}{\partial \beta} \times \frac{\beta}{R_0} = 1 > 0.$$

As we know, parameter β indicates the transmission rate of COVID-19. It showed that the relationship between β and R_0 gave a positive value. It revealed that if the parameter value were increased (decreased), the value of R_0 would also increase (decrease). If the values for other parameters were fixed, Figure 3 gives the relationship between β and R_0 .

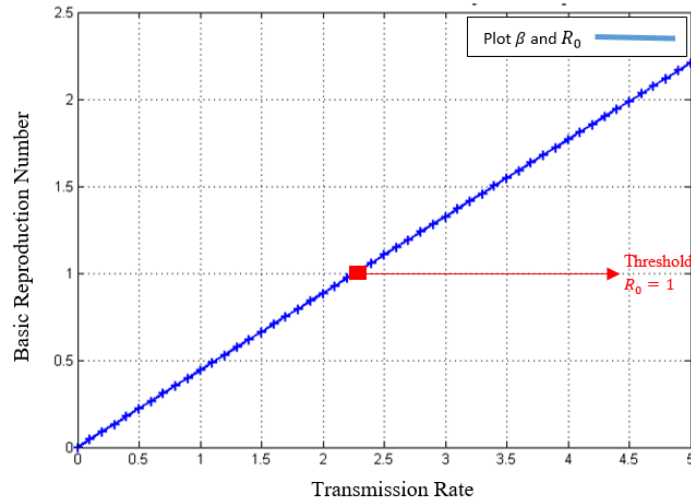


Figure 3. Sensitivity Analysis Parameter β to R_0 .

Figure 3 shows that a reduction in transmission rate will decrease the R_0 significantly, which relates to the infected case. In reality, this result can be interpreted as the transmission rate could be reduced by controlling interaction among people in the population by applying social and physical distancing. In addition, using a mask in the crowd could reduce the transmission rate of COVID-19.

- The sensitivity of parameter p with respect to R_0 is defined as

$$C_p^{R_0} = \frac{\partial R_0}{\partial p} \times \frac{p}{R_0} = -\frac{p}{1-p} < 0.$$

Parameter p is the tracing level of infected individuals. It resulted in a negative relationship. It means that if the value of the parameter p was increased (decreased), the value of R_0 will decrease (increase). If values for other parameters were fixed, the relationship between p and R_0 was given in Figure 4.

The tracing parameter explained the level of susceptible individuals who decide to have quarantine. We obtained sensitivity analysis that if more people were quarantined, then the R_0 decreased, related to infected cases. Since individuals in the quarantine compartment could not spread COVID-19 to others, the infected case would decrease. Furthermore, the combination of changes in the two parameters could also obtain various values of basic reproduction numbers. The result is given in Figure 5.

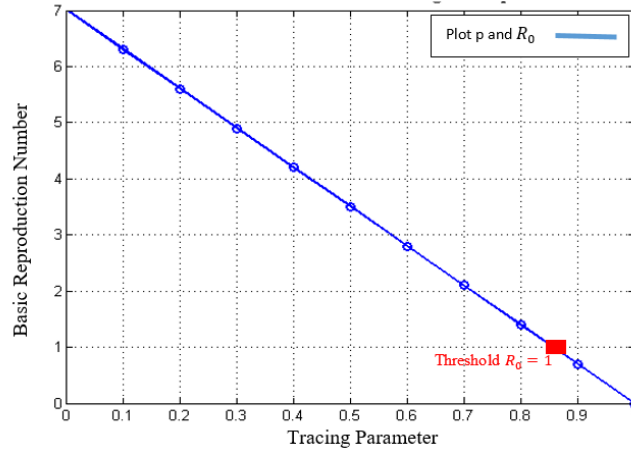


Figure 4. Sensitivity analysis parameter p to R_0 .

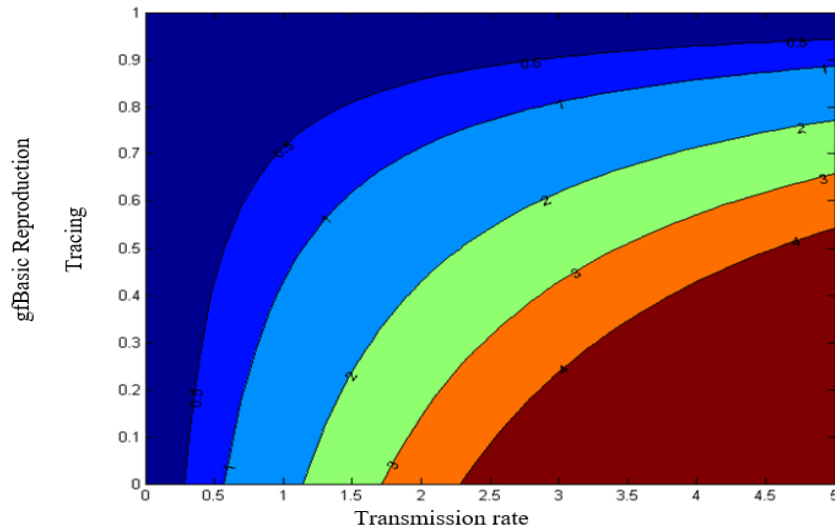


Figure 5. Relationship of parameter β and p with respect to the R_0 value.

4. NUMERICAL SIMULATION

4.1. Parameter Estimation

Estimation of parameter estimates population parameters using sample statistics. In this model, several parameters were estimated using actual data collected from the kawalcovid19.id website. Daily COVID-19 data for the West Sulawesi from September 1, 2021, to October 15, 2021. The estimation of parameter values was performed by minimizing the objective function of the multi-variable nonlinear function using the 'fmincon' toolbox in Matlab. This estimation minimized the objective function.

$$\min_{par=(\beta,p,\sigma,\gamma,\delta)} \|Z_{real} - Z_{model}\|.$$

In addition, we also estimated the fractional-order for the model. We used the Grunwald Letnikov method. The number of active cases is defined as

$$A = K - M - S,$$

where A is active case; K is a confirmed case; M is a death case, and S is a recovered case. The estimation of active cases COVID-19 for West Sulawesi was given in Figure 6.

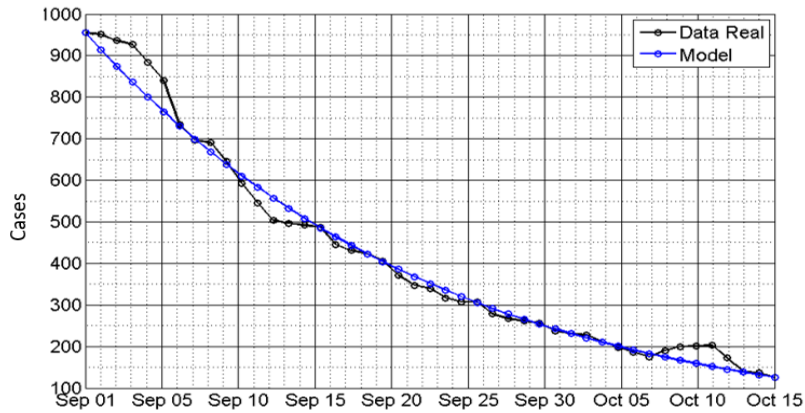


Figure 6. The estimation of active cases of COVID-19 in West Sulawesi.

Estimation results of the model parameter of the system (2) are given in Table 3. From these parameters, the R_0 for West Sulawesi is $R_0 = 1.765$ which means there is still potential for spreading the disease in a population. The estimation of fractional-order for West Sulawesi is $\alpha = 0.9394$. The number of active cases from several values of α were given in Figure 7.

Table 3. Parameter estimation of West Sulawesi.

Parameter	Value
μ	$4,21 \times 10^{-5}$
β	3.999
p	0.7477
σ	0.5
γ	0.0714
δ	0.052
α	0.9394

4.2. The scenario of Numerical Simulation

In this numerical simulation, several scenarios would be given by making adjustments to two parameters related to the COVID-19 model, namely β represents the transmission rate of infected individuals with susceptible individuals and p represents the proportion of tracing COVID-19.

4.2.1. Scenarios for contact transmission rates between infected individuals and susceptible individuals

In this simulation, we changed the value of β and showed the result related to R_0 . We fixed the value of other parameters to be constant. The result of Figure 8 shows the number of active cases of

COVID-19 in West Sulawesi with several values of the contact transmission rate. In general, three scenarios showed the same behavior. Scenario one was the number of active cases when the transmission value was reduced by 10% (Table 4). The number of cases decreased significantly in 20 days to 700 and declined to below 100 the following day. However, a difference occurred in scenario two and scenario three. Both scenarios showed a decrease to below 100 in 10 days. It showed that active cases become lower and decrease faster with the lower value of the contact transmission parameter.

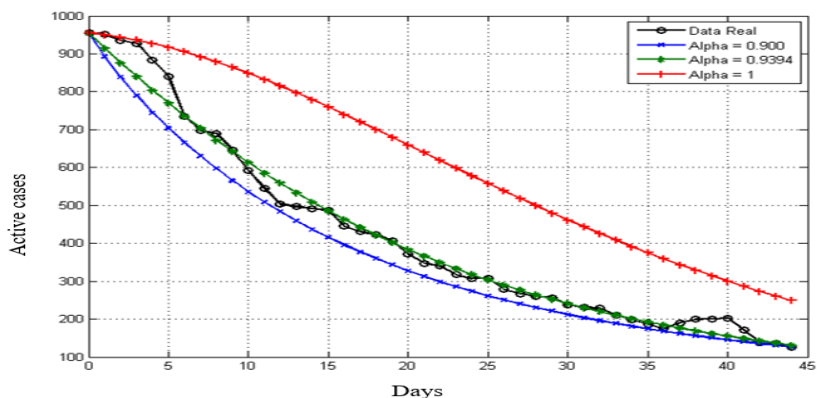


Figure 7. The number of active cases of COVID-19 in West Sulawesi using actual data and some fractional order α .

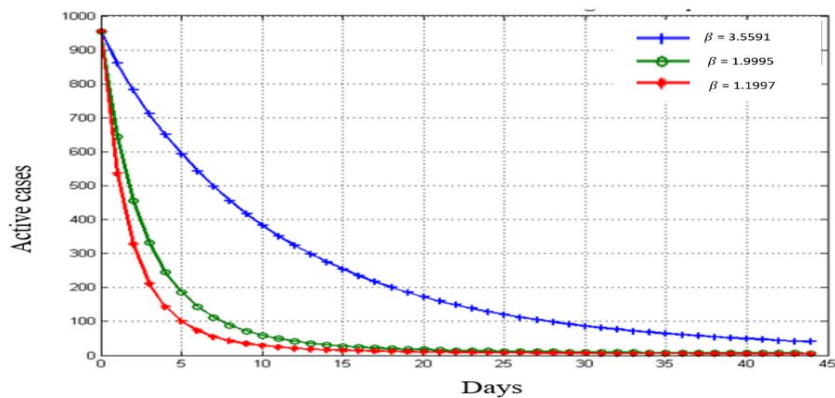


Figure 8. The number of active cases of COVID-19 in West Sulawesi with adjustment to the rate of transmission contact β for $\alpha = 0.9394$.

Table 4. The scenario of adjusting the contact transmission rate for the fractional-order COVID-19 spread model in West Sulawesi.

Parameter	Scenario 1 (Decrease β by 10%)	Scenario 2 (Decrease β by 50%)	Scenario 3 (Decrease β by 90%)
$\beta = 3.999$	3.5991	1.9995	1.1997
$R_0 = 1.765$	1.5888	0.8826	0.5296

4.2.2. Scenario to tracing proportion of COVID-19

From the estimation results, the parameter values for the proportion of traced infected individuals (p) equal 0.747. We fixed other parameters to be constant. Figure 9 shows the number of active cases of COVID-19 in West Sulawesi with different tracing proportions. In general, three scenarios showed the same behavior. Scenario 1 showed a decrease when the value of this parameter was increased by 2%. In 20 days, the number of active cases decreased to around 700. In 45 days, it was below 100. In scenario 2, it fell more rapidly than in scenario 1. Within 20 days, the number of active cases decreased to approximately 800. At 45 days, it was around 50 active cases. Scenario 3 has below 100 cases in 20 days and decreases until day 45. This simulation revealed that if the number of people who were traced and quarantined increases, it will reduce the number of active cases of COVID-19. We have the same result according to the results of the sensitivity analysis.

Table 5. The scenario of adjusting the tracing proportion for the fractional-order COVID-19 spread model in West Sulawesi

Parameter	Scenario 1 (Increase p by 2%)	Scenario 2 (Increase p by 5%)	Scenario 3 (Increase p by 10%)
$p = 0.747$	0.7619	0.7843	0.8217
$R_0 = 1.765$	1.6665	1.5097	1.2480

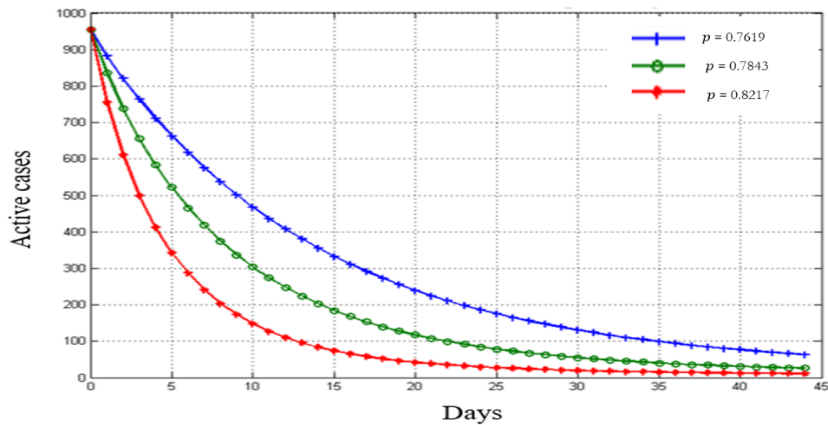


Figure 9. The number of active cases of COVID-19 in West Sulawesi with adjustment to tracing proportion p for $\alpha = 0.9394$.

5. CONCLUSIONS

The fractional-order that fits the data for West Sulawesi data is $\alpha = 0.9394$. From numerical simulations, we suggest several decisions to suppress the spread of COVID-19. The government may establish policies for applying PPKM to limit public interactions. If the interaction among individuals is restricted, then it will reduce the level of contact transmission. In other words, it can reduce the basic reproduction numbers and decrease infected cases. In addition, higher tracing of infected individuals and applying quarantine also reduce the number of infected COVID-19 in West Sulawesi.

REFERENCES

- [1] D. Aldila et al., “A mathematical study on the spread of COVID-19 considering social distancing and rapid assessment: The case of Jakarta, Indonesia,” *Chaos, Solitons & Fractals*, vol. 139, p. 110042, Jan. 2020, doi: 10.1016/j.chaos.2020.110042.
- [2] J. Chávez, T. Goetz, S. Siegmund, and K. Wijaya, “An SIR-Dengue transmission model with seasonal effects and impulsive control,” *Mathematical Biosciences*, vol. 289, Jan. 2017, doi: 10.1016/j.mbs.2017.04.005.
- [3] N. Chitnis, J. Hyman, and J. Cushing, “Determining Important Parameters in the Spread of Malaria Through the Sensitivity Analysis of a Mathematical Model,” *Bulletin of mathematical biology*, vol. 70, pp. 1272–1296, Jan. 2008, doi: 10.1007/s11538-008-9299-0.
- [4] N. 'Izzati Hamdan and A. Kilicman, “A fractional order SIR epidemic model for dengue transmission,” *Chaos, Solitons and Fractals*, vol. 114, Jan. 2018. doi: 10.1016/j.chaos.2018.06.031.
- [5] J. Zhang, J. Jia, and X. Song, “Analysis of an SEIR Epidemic Model with Saturated Incidence and Saturated Treatment Function,” *TheScientificWorldJournal*, vol. 2014, p. 910421, Jan. 2014, doi: 10.1155/2014/910421.
- [6] N. Anggriani, S. Toaha, and K. Kasbawati, “Optimal Control of Mathematical Models on The Dynamics Spread of Drug Abuse,” *Jurnal Matematika, Statistika dan Komputasi*, vol. 17, pp. 339–348, Jan. 2021, doi: 10.20956/j.v17i3.12467.
- [7] S. Sulma, S. Toaha, and K. Kasbawati, “Stability Analysis of Mathematical Models of the Dynamics of Spread of Meningitis with the Effects of Vaccination, Campaigns and Treatment,” *Jurnal Matematika, Statistika dan Komputasi*, vol. 17, pp. 71–81, Aug. 2020, doi: 10.20956/jmsk.v17i1.10031.
- [8] R. M. Muin, S. Toaha, and Kasbawati, “Effect of vaccination and treatment on the MSEICR model of the transmission of hepatitis B virus,” in *Journal of Physics: Conference Series*, Nov. 2019, vol. 1341, no. 6. doi: 10.1088/1742-6596/1341/6/062031.
- [9] H. Hartati, S. Toaha, and K. Kasbawati, “Stability analysis of SEISEIR-SEI modelling on the dynamics of spread dengue fever with vaccination and insecticide,” *Journal of Physics: Conference Series*, vol. 1341, p. 062033, Oct. 2019, doi: 10.1088/1742-6596/1341/6/062033.
- [10] S. Annas, M. Pratama, M. Rifandi, W. Sanusi, and S. Side, “Stability Analysis and Numerical Simulation of SEIR Model for pandemic COVID-19 spread in Indonesia,” *Chaos, Solitons & Fractals*, vol. 139, Jan. 2020, doi: 10.1016/j.chaos.2020.110072.
- [11] E. Iboi, C. Ngonghala, and A. Gumel, “Will an imperfect vaccine curtail the COVID-19 pandemic in the U.S.?” *Infectious Disease Modelling*, vol. 5, Jan. 2020, doi: 10.1016/j.idm.2020.07.006.
- [12] S. Mwalili, M. Kimathi, V. Ojiambo, D. Gathungu, and R. Mbogo, “SEIR model for COVID-19 dynamics incorporating the environment and social distancing,” *BMC Research Notes*, vol. 13, Jan. 2020, doi: 10.1186/s13104-020-05192-1.
- [13] F. Ndairou, I. Area, J. Nieto, and D. F. M. Torres, “Mathematical Modeling of COVID-19 Transmission Dynamics with a Case Study of Wuhan.” Jan. 2020.
- [14] O. Zakary, B. Sara, M. Rachik, and H. Ferjouchia, “Mathematical Model to Estimate and Predict the COVID-19 Infections in Morocco: Optimal Control Strategy,” *Journal of Applied Mathematics*, vol. 2020, pp. 1–13, Jan. 2020, doi: 10.1155/2020/9813926.
- [15] E. Bas, B. Acay, and R. Ozarslan, “Fractional models with singular and non-singular kernels for energy efficient buildings,” *Chaos: An Interdisciplinary Journal of Nonlinear Science*, vol. 29, no. 2, p. 23110, 2019, doi: 10.1063/1.5082390.

- [16] F. Ndairou, I. Area, J. Nieto, C. Silva, and D. F. M. Torres, “Fractional model of COVID-19 applied to Galicia, Spain and Portugal,” *Chaos, Solitons & Fractals*, vol. 144, p. 110652, Jan. 2021, doi: 10.1016/j.chaos.2021.110652.
- [17] N. Ozalp and E. Demirci, “A fractional order SEIR model with vertical transmission,” *Mathematical and Computer Modelling*, vol. 54, pp. 1–6, Jan. 2011, doi: 10.1016/j.mcm.2010.12.051.
- [18] K. Saad, “Fractal-fractional Brusselator chemical reaction,” *Chaos Solitons & Fractals*, vol. 150, p. 111087, Jan. 2021, doi: 10.1016/j.chaos.2021.111087.
- [19] B. Tang, “Dynamics for a fractional-order predator-prey model with group defense,” *Scientific Reports*, vol. 10, Jan. 2020, doi: 10.1038/s41598-020-61468-3.
- [20] J. F. Gómez-Aguilar, J. Rosales, and M. Guía, “RLC electrical circuit of non-integer order,” *Central European Journal of Physics*, vol. 11, Jan. 2013, doi: 10.2478/s11534-013-0265-6.
- [21] S. Müller, M. Kästner, J. Brummund, and V. Ulbricht, “A nonlinear fractional viscoelastic material model for polymers,” *Computational Materials Science - COMPUT MATER SCI*, vol. 50, pp. 2938–2949, Jan. 2011, doi: 10.1016/j.commatsci.2011.05.011.
- [22] S. Suriani, S. Toaha, and K. Kasbawati, “MSEICR Fractional Order Mathematical Model of The Spread Hepatitis B,” *Jurnal Matematika, Statistika dan Komputasi*, vol. 17, pp. 314–324, Dec. 2020, doi: 10.20956/jmsk.v17i2.10994.
- [23] S. Y. Chae *et al.*, “Estimation of Infection Rate and Predictions of Disease Spreading Based on Initial Individuals Infected With COVID-19,” *Frontiers in Physics*, vol. 8, Aug. 2020, doi: 10.3389/fphy.2020.00311.
- [24] I. Podlubny, “Chapter 2 - Fractional Derivatives and Integrals,” in *Fractional Differential Equations*, vol. 198, I. Podlubny, Ed. Elsevier, 1999, pp. 41–119. doi: [https://doi.org/10.1016/S0076-5392\(99\)80021-6](https://doi.org/10.1016/S0076-5392(99)80021-6).
- [25] I. Petráš, “Fractional-Order Systems,” in *Fractional-Order Nonlinear Systems: Modeling, Analysis and Simulation*, Berlin, Heidelberg: Springer Berlin Heidelberg, 2011, pp. 43–54. doi: 10.1007/978-3-642-18101-6_3.
- [26] M. Tavazoei and M. Haeri, “A necessary condition for double scroll attractor existence in fractional-order systems,” *Physics Letters A*, vol. 367, pp. 102–113, Jan. 2007, doi: 10.1016/j.physleta.2007.05.081.
- [27] M. Wu, Z. Yang, and W. Lin, “Exact asymptotic stability analysis and region-of-attraction estimation for nonlinear systems,” *Abstract and Applied Analysis*, vol. 2013, 2013, doi: 10.1155/2013/146137.
- [28] E. Ahmed, A. El-Sayed, and H. El-Saka, “On some Routh-Hurwitz conditions for fractional order differential equations and their applications in Lorenz, Rössler, Chua and Chen systems,” *Physics Letters A*, vol. 358, pp. 1–4, Jan. 2006, doi: 10.1016/j.physleta.2006.04.087.
- [29] D. Matignon, “Stability Results For Fractional Differential Equations With Applications To Control Processing,” vol. 2, Jan. 1997.
- [30] I. Dzhalladova and M. Růžičková, “Stability of The Equilibrium of Nonlinear Dynamical Systems,” *Tatra Mountains Mathematical Publications*, vol. 71, pp. 71–80, Jan. 2018, doi: 10.2478/tmmp-2018-0007.
- [31] S. Choi, B. Kang, and N. Koo, “Stability for Caputo Fractional Differential Systems,” *Abstract and Applied Analysis*, vol. 2014, pp. 1–6, Jan. 2014, doi: 10.1155/2014/631419.
- [32] P. Dreessche and J. Watmough, “Reproduction Numbers and Sub-threshold Endemic Equilibria for Compartmental Models of Disease Transmission,” *Mathematical Biosciences*, vol. 180, pp. 29–48, Jan. 2002, doi: 10.1016/S0025-5564(02)00108-6.